29th EPS Conference on Plasma Phys. and Contr. Fusion Montreux, 17-21 June 2002 ECA Vol. **26B**, P-4.059 (2002)

# Global Gyrokinetic Simulations of Nonlinear Interaction of Zonal Flows with ITG Modes

S.J. Allfrey, R. Hatzky[1], A.Bottino and L.Villard

*Centre de Recherches en Physique des Plasmas, Association EURATOM-Confédération Suisse, EPFL, 1015 Lausanne, Switzerland*

[1]*Max-Planck-Institut für Plasmaphysik, Teilinstitut Greifswald, D-17491 Greifswald, Germany*

## 1. Introduction

The $\delta f$ particle-in-cell (PIC) method provides an approach to solving the nonlinear gyrokinetic equations governing the ion-temperature-gradient-driven (ITG) instabilities commonly held responsible for core plasma transport. The method is, however, rather demanding with respect to current typically available computational resources. The TORB[1] code implements this method in a straight $\Theta$-pinch geometry. The code now employs an adiabatic electron response within surfaces of constant $r$. Thus the equations governing the $m_\theta = 0, n_z = 0$ Fourier component of the electrostatic potential, $\phi_{00}$, which gives rise to zonal $\mathbf{E} \times \mathbf{B}$ flows, are as for the case of finite rotational transform. The underlying equations obey an energy conservation principle allowing for an intrinsic check on the quality of simulation. This has been well satisfied ($\sim$20% deep into the nonlinear stage) though optimising the phase space sampling provided by the markers.

## 2. The model

Under the geometry considered the equations of motion are

$$\frac{d\mathbf{R}}{dt} = v_{\|}\mathbf{e}_{\|} - \frac{\nabla\langle\phi\rangle}{B} \times \mathbf{e}_{\|} \ , \tag{1}$$

$$\frac{dv_{\|}}{dt} = -\frac{\Omega_i}{B}\,\mathbf{e}_{\|} \cdot \nabla\langle\phi\rangle \ . \tag{2}$$

Along these characteristics $\delta f$ evolves according to

$$\frac{d\,\delta f}{dt} = -f_0 \left[\frac{\langle\mathbf{E}\rangle \times \mathbf{e}_{\|}}{B} \cdot \frac{\nabla f_0}{f_0} + \frac{\Omega_i}{B}\mathbf{e}_{\|} \cdot \langle\mathbf{E}\rangle \frac{1}{f_0}\frac{\partial f_0}{\partial v_{\|}}\right] . \tag{3}$$

The quasineutrality equation with linearised polarisation density is

$$\langle n_i\rangle - \ n_0 = \frac{e n_0}{T_e}\left(\phi - \bar{\phi}\right) - \nabla_\perp \left(\frac{n_0}{B\Omega_i}\nabla_\perp \phi\right) \ . \tag{4}$$

Here $\Omega_i = q_i B/m_i$ is the ion cyclotron frequency, $\langle\phi\rangle$, $\langle\mathbf{E}\rangle$ and $\langle n_i\rangle$ and the gyro-averaged potential, electric field and ion density and , $\bar{\phi}$ is the magnetic surface average of the potential. The quantity $\bar{\phi}$ is given by $\phi_{00}$ in this geometry. The quasineutrality equation is subject to the boundary conditions,

$$\frac{\partial}{\partial r}\phi_{n,m=0}\bigg|_{r=0} = \quad \phi_{n,m\neq 0}\bigg|_{r=0} = \quad \phi\bigg|_{r=r_a} = 0, \tag{5}$$

which simply impose a vanishing tangential electric field at $r_a$, the outer boundary of the plasma. Retaining the parallel nonlinearity in equation (1) allows for an energy conservation principle to be satisfied

$$\frac{d}{dt}(\mathcal{E}_{kin} + \mathcal{E}_{field}) = 0 \ , \tag{6}$$

$$\mathcal{E}_{kin} = \int \frac{1}{2} m_i v^2 f \, d\mathbf{R} d\mathbf{v} \qquad \mathcal{E}_{field} = \int \frac{q_i}{2} \left( \langle n_i \rangle - n_0 \right) \phi \, d\mathbf{x} \ . \tag{7}$$

## 3. Results

The simulations used 134 million ($2^{27}$) markers over a cubic finite element basis of dimension $n_r = 64, n_\theta = 256, n_z = 32$. The time step was $\Delta t = 40\Omega_i$. Fourier modes in $\theta$ and $z$ in the range $-96 \leq m \leq 96$ and $0 \leq n \leq 6$ were retained in the filter. The initial ion temperature profile $T_i(r)$ is show in figure 3. A flat density ($n_0$) and electron temperature profile ($T_e = T_i(0.5) = 5keV$), were used. The radius of the pinch was $r_a = 135\rho_{i0}$ and the periodicity length $20\pi r_a$ with $\rho_{i0}$ the thermal Larmor radius at $r = 0.5$. The magnetic field was taken as 2.5T and the ions to be deuterium, $q_i/m_i = 4.79 \times 10^7 C/kg$, giving $\Omega_i = 1.20 \times 10^8$ s.

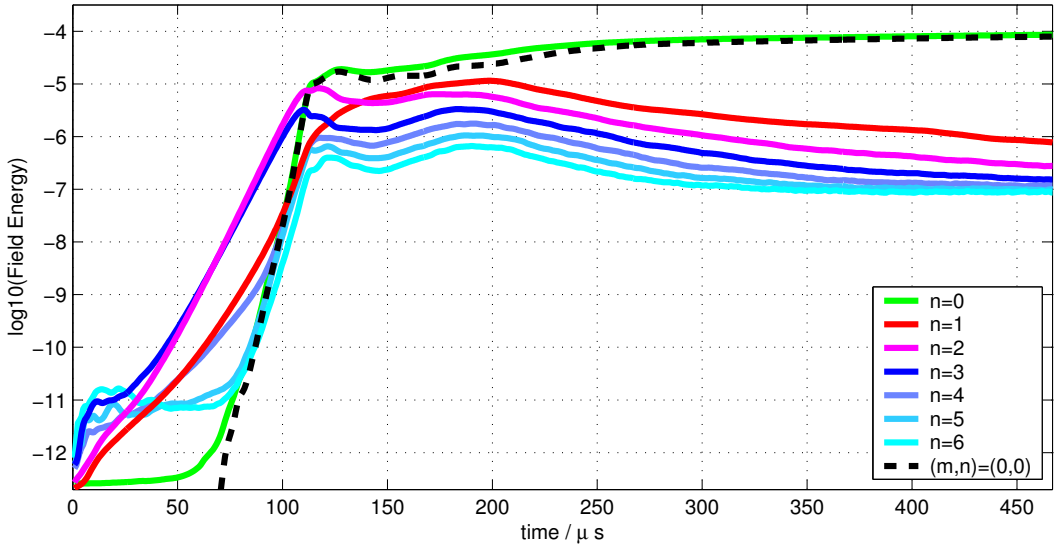


Figure 1. A log plot of the Fourier decomposition of the electrostatic field energy vs. time

Figure 1 shows the evolution of the ITG turbulence toward a saturated nonlinear state. The most unstable linear modes are in the ranges $(n, m) = (2, \sim 48), (3, \sim 55), (1, \sim 30)$ and $(4, \sim 60)$, with $n = 0, 5$ and 6 linearly stable. Initially we see just the linear instabilities, but at $60\mu$s the nonlinear destabilisation of $n = 0, 5$ then 6 begins. Nonlinear feedback begins with a first roll over at $100\mu s$ followed by a second at $200\mu s$. Finally past $400\mu$s the system is seen to be approaching a steady state with the expected inverse cascade in $n$ dominated by an $(n, m) = (0, 0)$ mode.

The top two traces in figure 2 show the absolute values of kinetic and electrostatic energy of the perturbation. By equation 6 they should be equal for a perfect simulation. Energy is seen to be well conserved with a relative error of $\sim 33\%$ at the end of the simulation. The Fourier filter contains $\geq 98\%$ of the signal throughout the nonlinear phase.

Seen in the bottom trace of figure 2 is the heat flux,

$$Q = \frac{1}{V} \int \frac{1}{2} m_i v^2 \frac{\langle \mathbf{E} \rangle \times \mathbf{e}_{\|}}{B} \cdot \frac{\nabla r}{|\nabla r|} f \, d\mathbf{R} d\mathbf{v} \tag{8}$$

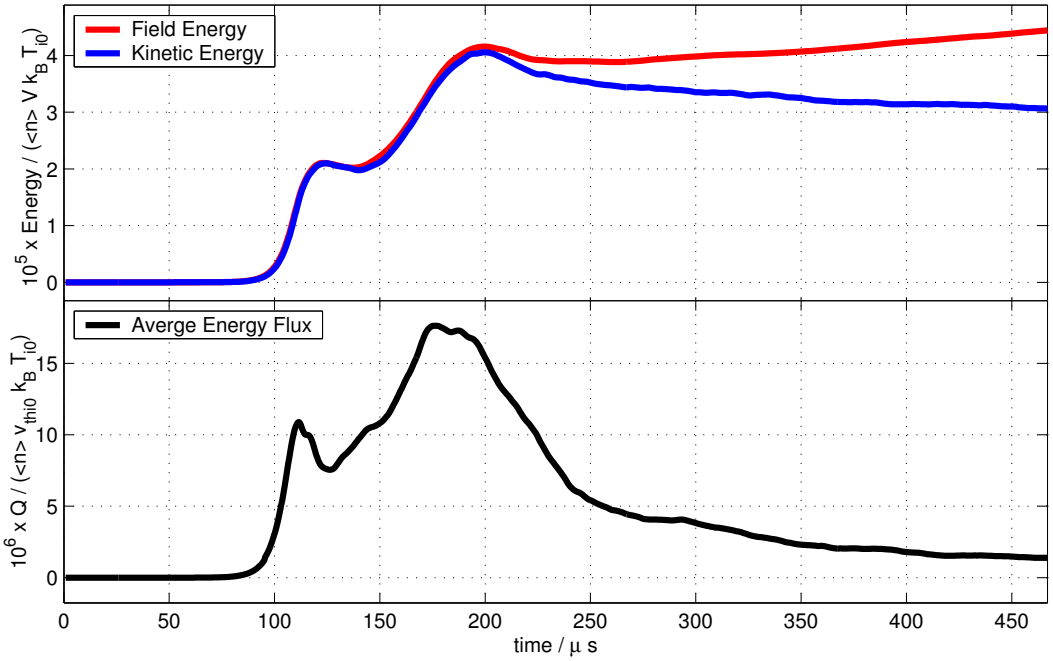


Figure 2. Top, the absolute value of the kinetic and electrostatic field energy (eq.7) of the perturbation normalised to the thermal energy of the plasma and bottom, the normalised average radial energy flux Q (eq.8) vs. time

Previous equivalent simulations [1] did not retain the $\bar{\phi}$ term in equation 4, corresponding to a volume adiabatic electron response. In the previous simulations $Q$ in the late nonlinear stage was an order of magnitude larger than the value found here, with the field energy of comparable magnitude. This is due to fact the the electron model used now allows for the generation of zonal flows [3].

Figure 3 shows the radial profiles at $470\mu s$. In orange and blue are shown the initial and final effective temperature $T_{eff} = \langle v_{thi}^2 \rangle$ profiles. What is immediately striking are the plateau regions of low gradient/ high transport directly, corresponding with the regions of ITG turbulence which are shown in red. In black is shown $-\partial\Phi_{00}/\partial r$ which is proportional to the zonal $\mathbf{E} \times \mathbf{B}$ flow.

We now describe in detail the evolution of the radial envelope of ITG modes. In the linear stage the ITG modes are centred around the maximum temperature gradient at $r = 0.5$. As the modes spread radially and increase in magnitude the zonal flow becomes strong enough to shear the primary ITG envelope radially in two. This is responsible for the first roll over at $100\mu s$ seen in figure 1. This region now settles into an essentially steady state consisting of a central positive flow region in which ITG modes are suppressed, flanked by two bands of negative flow in which they persist. The evolution continues on the inner and outer boundaries of this envelope, where the initial sequence of events is repeated, the roll over at $200\mu s$, leading now to four regions of ITG activity. At $470\mu s$ this bifurcation process is in the course of repeating itself once more, with the splitting more advanced on the outer boundary.

We note that not only are the ITG convective cells restricted to the $\mathbf{E} \times \mathbf{B}$ stream they lie in (shear flow suppression), they are suppressed throughout those streams rotating in a positive sense. In purple is shown a histogram of the heat flux $Q$ in $5$ radial bins. It is clear that it is only at the boundaries of the ITG turbulence, which are still evolving, that a significant flux is driven. In the middle of the envelope (bins $3$ and $4$) the flux levels have remained at a constant

low level since $\sim 380\mu s$ having peaked $\sim 200\mu s$ earlier. Presumably the large fluxes seen at boundaries will follow the same behaviour as the entire radial interval reaches saturation.

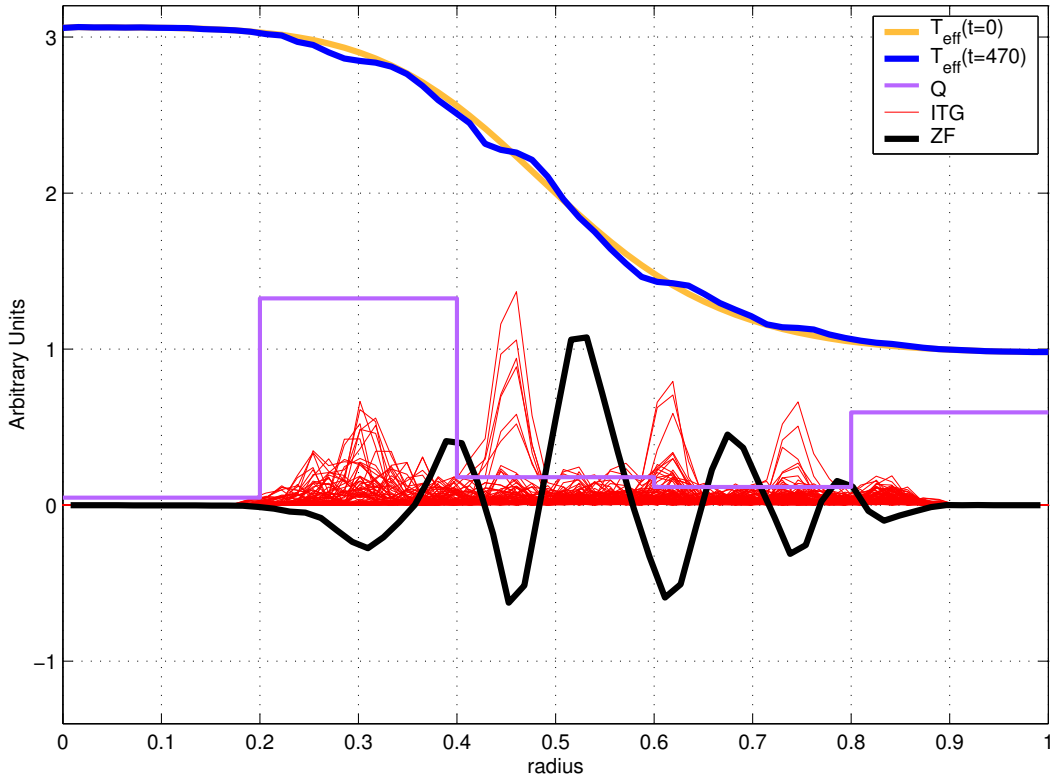


Figure 3. Radial profiles of the effective temperature $T_{eff}$, ITG mode spectrum, $\mathbf{E} \times \mathbf{B}$ zonal flow and binned heat flux Q. . Profiles have been rescaled for illustrative purposes

## 4. Conclusions

We have presented simulation of the suppression of ITG driven turbulence by zonal flows in straight $\Theta$-pinch geometry with very good energy conserving properties. The system is seen to approach a steady state in the absence of any collisional terms. The use of an optimised phase space sampling is crucial in attaining energy conservation. Finite rotational transform needs to be introduced to be consistent with the electron model used. Further simulations will examine the dependence of the radial scale-length of the zonal flows and the concomitant scaling of driven flux.

*This work was partly supported by the Swiss National Science Foundation. Simulations were executed on the IBM Regatta of the Rechenzentrum, Max-Planck-Gesellschaft, Garching and the SGI Origin 3800 of the Ecole Polytechnique Fédérale de Lausanne.*

### References

[1] R. Hatzky, T.M. Tran, A. Könies, R. Kleiber, and S.J. Allfrey, Phys. Plasmas **9**, 898 (2002).

[2] L. Villard, A. Bottino, O. Sauter and J. Vlaclavik, Phys. Plasmas **9**, June (2002).

[3] A. Hasegawa, C.G.Maclennan and Y.Kodama, Phys. Fluids **27**, 2122 (1979)